Use of laser-produced soft x rays for the production of excited metastable ions

R. G. Caro, J. C. Wang,* J. F. Young, and S. E. Harris
Edward L. Ginzton Laboratory, Stanford University, Stanford, California 94305
(Received 20 December 1983)

A detailed investigation is presented of the use of soft x rays, emitted from a laser-produced plasma, for the excitation of highly energetic ions. The emphasis is on the excitation of $Li^+(1s\,2s)$ metastable levels with energies of approximately 60 eV. The experiments were made possible by the use of a geometry in which the laser beam was focused through the Li vapor onto a massive target placed inside the vapor. Populations of $Li^+(1s\,2s)$ ions in excess of 10^{15} cm^{-3} have been measured and the effect of varying parameters such as laser energy, distance from the target, Li density, and time delay after the initial excitation has been examined. In this work the plasma emission can be considered as radiation from a blackbody with a temperature of 10—100 eV, and the conversion efficiency from 1.06-μm radiation to blackbody radiation was estimated to be in excess of 5%. A comparison has been made of the effect of using Q-switched ($\tau\sim 10$ ns, $E\sim 200$ mJ) and actively mode-locked ($\tau\sim 0.6$ ns, $E\sim 50$ mJ) neodymium-doped yttrium aluminum garnet (Nd:YAG) lasers to make the soft-x-ray—emitting plasma. $Li^+(1s\,2s)$ population measurements have been made for the cases of Ta, Fe, Ni, and Li target materials, and the populations excited by photoelectrons into the $Li(1s^2 2p)$ and $Li^+(1s^2)$ levels have been measured. The applications of these experiments to various proposed extreme-ultraviolet laser systems are discussed.

I. INTRODUCTION

When high-power laser radiation is focused onto a target, a plasma is formed which has dimensions characteristic of the laser focal spot. For 1.06-μm laser intensities of approximately 10^{13} W cm^{-2}, the plasma can be described, by a simple hydrodynamic model,[1] as a rapidly expanding hemisphere. The outer portions of this plasma have an electron density which corresponds to a plasma frequency equal to the frequency of the incident laser radiation. The electrons heat—and the laser radiation is absorbed—by inverse bremsstrahlung while, for high Z targets, the plasma emission is primarily due to free-bound recombination and to line radiation.[2,3] For a tantalum target, such as is used in this work, the continuum radiation dominates over the line radiation.[3] The emitted spectrum can thus be approximated by that of a blackbody with an appropriate temperature which, for these experiments, is believed to be between 10 and 100 eV. The conversion efficiency from 1.06-μm laser energy to emitted soft x-ray energy can readily be between 10% and 50% for high Z targets.[4] Even with laboratory-scale lasers ($\lesssim 1$ GW), soft x-ray power densities in excess of 1 GW cm^{-2} can be produced at distances of several millimeters from the plasma core.

In this paper we study the use of laser-produced soft x rays to produce large densities ($>10^{15}$ cm^{-3}) of excited metastable ions;[5] in particular, $Li^+(1s\,2s)^3S$ and $Li^+(1s\,2s)^1S$ which have energies relative to their ground levels of 59.0 and 60.9 eV, respectively. These metastable ions have been excited by photoionization of $Li(1s^2 2s)^2S$ atoms by the soft x rays emitted from a laser-produced plasma. Metastable ions of this type are of interest as energy storage levels for xuv lasers and xuv radiation sources, and also as primary species for the study of collision kinetics and reactions in the energy range from 30 to 300 eV.

The use of laser-produced incoherent x rays for inner-shell ionization and production of excited radiating ions was first suggested by Duguay and Rentzepis.[6] Mani, Hyman, and Daugherty[7] suggested that the requirement for very short laser pulses and high peak powers of soft x-ray radiation could be made less stringent by, instead, producing metastable ions. Although extensive theoretical discussion of the use of laser-produced plasmas as x-ray sources for the excitation of xuv laser systems has appeared in the literature,[8–12] until recently only a single attempt[10] had been made to investigate such a procedure experimentally.

The xuv laser proposals mentioned so far have involved various combinations of thin-foil targets, and filter foils designed to separate the x-ray source from the region to be pumped and to modify the x-ray spectrum. The lack of experimental results seems likely to be due, to a large extent, to the complexity of such configurations and to the inconvenience of a geometry in which the filter foil would be destroyed by every shot. To circumvent these problems, an experimental geometry has been used in this work whereby a massive target was placed inside, and was surrounded by, the ambient Li vapor (Fig. 1). A Nd:YAG laser beam was focused through the Li vapor to a spot size of approximately 20 μm on the target and a plasma was produced. Soft x rays were emitted from the plasma and propagated into the surrounding vapor with the consequent inner-shell photoionization of the ambient Li atoms.

The laser beam, propagating through the Li vapor at an intensity of approximately 10^{13} W cm^{-2}, will completely ionize the vapor. This will, in principle, affect the focusing of the beam on target. There are two primary contributions to the change in refractive index which is seen by

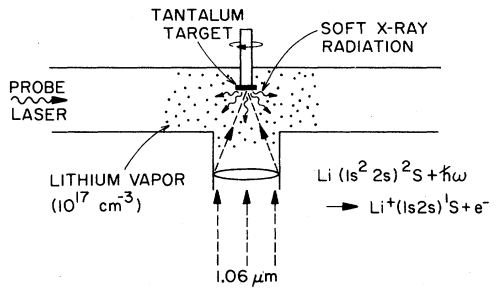

FIG. 1. Schematic of experimental configuration.

the propagating laser beam. For Li, at a wavelength of 1.06 μm, these result from the reduction of the normal index caused by the removal of ground-state neutrals, and from the addition of a negative increment caused by the formation of the plasma. Both contributions (which in this case have a ratio of about 3.3 to 5) act to defocus the beam. Although we have not studied the problem in detail, a rough calculation indicates that defocusing should become noticeable at an ambient Li density somewhere between 10^{17} and 10^{18} atoms cm^{-3}.

This paper addresses such questions as: How large a metastable ion density can be produced by photoionization by laser-produced soft x rays; what are the functional dependences of the metastable density on factors such as the distance from the target and the Li density; and how long do the excited metastables last? In Sec. II the experimental details of this work are described, while in Sec. III the experimental results are presented. Section IV is devoted to a summary and a discussion of the implications of this work to possible xuv laser systems.

II. EXPERIMENTAL DETAILS

A. The target cell

In Fig. 2 is shown the target cell used in this work. The cell was a five-arm heat pipe[13] constructed from one-inch diameter stainless-steel tubing and lined with stainless-steel mesh which acted as a "wick." The target material was attached to the end of a hollow stainless-steel rod which was inserted into one arm of the heat pipe. The laser beam passed through a lens, entered the cell window opposite the "target" arm, and was focused onto the target which was positioned at the center of the five-arm cell. The targets used were of various materials and were machined flat normal to the direction of incidence of the laser beam. In order to expose a fresh surface of the target to the laser beam every few shots, the target "rod" was slowly rotated by means of a small electric motor. The rotating rod entered the cell through a ferrofluidic bearing seal.

This cell operated satisfactorily in a "heat pipe mode" up to Li densities of 10^{17} cm^{-3}. Since the target was positioned at the center of the cell, a probe laser could be passed at varying distances from the target through the region of Li vapor pumped by the x rays. The fifth, vertical arm of the cell allowed visual observation of the plasma. In order to prevent liquid Li from condensing on the target, it was found necessary to insert a separate heater into the target rod to heat the target to a temperature of 20–50 °C above that of the ambient Li vapor.

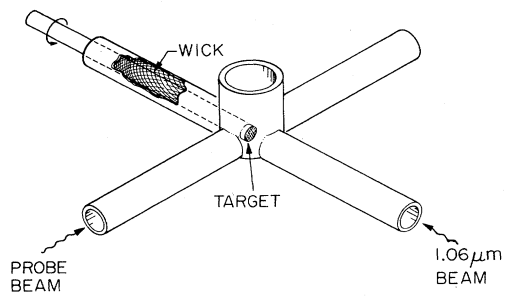

FIG. 2. Target cell.

B. The imaging system

It is desirable to have a means of monitoring and controlling the focusing of the plasma-producing laser beam. To this end we have used an imaging system which provided an image on a television screen of the 1.06 μm scattered light from the plasma. The size of this image was a measure of the focal spot size of the laser beam, while the intensity of the image was a rough measure of the reflectivity of the plasma.

This imaging system is illustrated in Fig. 3. The scattered light from the plasma reflected from a beam splitter (BS) and a one-to-one image of the scattering source was formed by a lens, L_1 in plane A. A graticule with 100 μm calibration marks was placed in plane A and this, together with the image of the scattered source, was magnified by a factor of approximately 20 and imaged onto an infrared-sensitive television camera by means of a microscope objective (OL). As the laser focusing lens (FL) was adjusted, the size of the image from the imaging system varied as did the intensity of the image.

This simple system proved extremely useful for locating the focal plane of lens FL and enabled constant experimental conditions to be maintained. It also allowed the authors to monitor the presence of effects such as beam defocusing by the Li vapor or the condensation on the target of liquid Li which resulted in greatly increased reflectivity of the 1.06 μm light from the plasma.

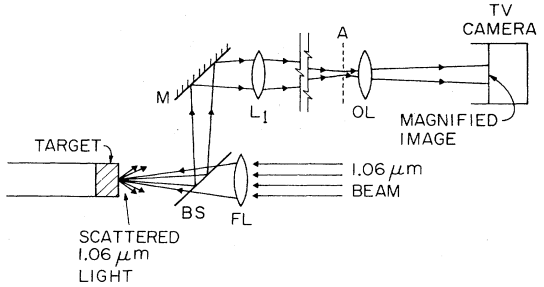

FIG. 3. Imaging systems: BS, beamsplitter; FL, focusing lens; M, mirror; L_1, transfer lens; OL, microscope objective.

C. The laser system

In Fig. 4 is shown a schematic illustration of the laser system used in this work. The heart of the system was an actively mode-locked Nd:YAG oscillator.[14] A Pockels cell was used to select a single pulse from the output pulse train. This pulse was amplified by three Nd:YAG rod amplifiers and then split into two beams. The weaker of these passed through a Faraday isolator, to decouple the system from the target, and was amplified in a final 6-mm-diameter rod amplifier to become the main 1.06 μm beam. This beam had a maximum energy of 100 mJ and a pulse duration of 600 ps. The more intense of the two beams was passed through frequency-mixing crystals to produce harmonics of the 1.06 μm laser beam. These were used to pump the amplifiers of the dye laser system shown in Fig. 4. The output from this second beam line was a pulse of somewhat less than 600 ps in duration with an energy of either 20 mJ at 532 nm or 2—3 mJ at 355 nm. The repetition rate of the system was 2 Hz.

A separate unstable-resonator Q-switched Nd:YAG laser was used to pump a grazing-incidence grating configuration dye laser oscillator. The output from this dye laser oscillator was a pulse of approximately 5 ns duration with a linewidth of 0.1—0.3 cm^{-1} depending on the wavelength being generated. This pulse was amplified by a series of two transversely pumped dye amplifiers and a final longitudinally pumped dye power amplifier. These amplifiers were pumped by the second beam from the main actively mode-locked Nd:YAG laser system. Thus, although the dye laser oscillator pulse had a duration of 5 ns, gain was only present in the dye amplifiers for approximately 600 ps. The final output was a tunable pulse which had a duration of 600 ps with a 5 ns "pedestal" which contained a total energy of less than 0.5% of that which was in the main pulse. A typical output energy of the system was 1—2 mJ for dyes pumped by 532 nm radiation. The linewidth of the pulse remained at the 0.1—0.3 cm^{-1} linewidth determined by the oscillator.

An advantage of this system was that it allowed the convenience and narrow linewidth of the grazing-incidence grating configuration dye laser oscillator to be combined with a short pulse output. However, due to longitudinal mode beating in the Q-switched Nd:YAG laser, the dye laser oscillator exhibited rapid intensity fluctuations during the 5 ns pulse which were very nonrepeatable. This resulted in drastic energy fluctuations in the output of the amplifier chain from shot to shot. To eliminate this problem, the system was set up so that the dye beam was close to saturation intensity at the input of the power amplifier, even for the smallest of oscillator signals. In this way, gain saturation acted to compensate for the intensity fluctuations in the dye laser oscillator and the output from the system exhibited only the $\pm 10\%$ energy fluctuations characteristic of the output from the actively mode-locked laser system.

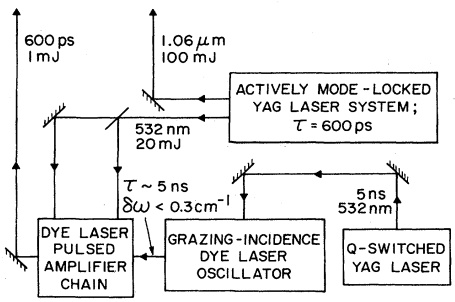

FIG. 4. Laser system.

In the majority of experiments, the main beam from the actively mode-locked laser system was focused onto the target in the experimental cell. The output from the dye laser was then passed through the probe arms of the cell to sample the photoionized Li population at a chosen distance from the target.

D. Population measurement techniques

To measure the population in an excited state of Li or Li^+ in the region which was pumped by x rays from the laser-produced plasma, the probe laser was passed through the region of interest and tuned through a strong transition originating on the appropriate excited level. At frequencies around this transition, the refractive index of the medium is dependent on the population in the excited state under consideration. Thus, knowledge of either the real or imaginary parts of the refractive index of the medium can be converted to a measurement of the population in the excited state.

In order to examine the absorption of the probe beam as its frequency was tuned through the transition, a portion was split off and used as a reference beam. The energies in both the reference beam and the transmitted beam were recorded by photodiodes and the ratio of the two signals was taken electronically to minimize the effect of fluctuations in the probe beam intensity. After averaging over 1—10 shots, absorption signals as small as 5% could be measured. By comparing the absorption traces with theoretical fits using numerically generated Voigt profiles, measurements of the number-density-length product, N^*L, of excited atoms could be deduced with an estimated accuracy of a factor of 2.

This procedure, however, requires some knowledge of the magnitude of the dominant Lorentzian component of the transition linewidth. An alternative method is to examine the real part of the refractive index, many linewidths from line center where the dependence on linewidth vanishes. To do this, the probe beam was split into two beams of equal intensity which were then recombined at the output of a Mach-Zehnder interferometer. The cell was placed in one arm of the interferometer and the probe laser was tuned through the transition from the excited state while the output of the interferometer was monitored.

The details of this interferometric measurement technique are discussed elsewhere,[15,16] but, conceptually, this technique is analogous to the well-known Rozhdestvenskii Hook method.[17] This technique is less sensitive than the absorption measurement outlined above, but requires no prior knowledge of transition linewidths and yields values of N^*L accurate to $\pm 20\%$ without great difficulty. In

this work these two techniques have been found to be complementary. It should be noted that, while the interferometric technique yields a measure of N^*fL, where f is the transition oscillator strength, the absorptive method yields a measurement of $(N^*fL)\delta\omega_L$ for optically thick samples. Thus, by comparing results obtained by these two methods, the Lorentzian linewidth of the transition, $\delta\omega_L$ can be deduced. It will be seen later that this can be used to obtain a measurement of the density of the Li^+ ground-state ion density.

III. EXPERIMENTAL RESULTS

A. Initial investigation

The work reported here consists of two separate series of experiments. In the initial series, reported briefly in Ref. 5, the beam from the actively mode-locked Nd:YAG laser was focused onto a Ta target, in the experimental cell of Fig. 2, by a lens of 12-cm focal length and an effective f number of $f/8$. The laser beam had a maximum energy of 100 mJ, of which 70% was contained in a main pulse with a measured duration of 600 ps. Leakage through the Pockels cell pulse selector resulted in a prepulse and two postpulses, each separated by 4 ns, 600 ps long, and containing approximately 10% of the total pulse energy.

Using a scanning knife edge, the beam radius in the focal plane and the effective confocal parameter were measured. At a total laser energy of 50 mJ, these were $\omega_0 \sim 20$ μm and $b \sim 900$ μm. These beam parameters imply an on-target intensity in the main pulse of approximately 10^{13} W cm^{-2}. At a distance of 1 mm from the target, the laser spot size is of the order of only 50 μm. Even at a distance of 7 mm, the laser spot size is approximately 0.4 mm. The region of Li vapor which interacts with the plasma-producing laser is thus an insignificant fraction of that considered in this work.

For this series of experiments no imaging system was used to monitor the laser plasma and the position of the focus was set by visual observation of the plasma. The rotation speed of the target corresponded to approximately 700 laser shots per revolution and a fresh section of the target was presented to the laser beam every 2–3 shots.

An energy-level diagram of Li and Li^+ is shown in Fig. 5(a). In the experiments described here, the spectrum of a blackbody with a radiation temperature of approximately 30 eV appears to adequately describe the emission from the laser-produced plasma. In Fig. 5(b) is shown the spectral emission from such a blackbody together with the photoionization cross sections of the inner and outer shells of Li.[18,19] At its peak at 60 eV, the cross section for inner-shell photoionization[18] of Li atoms is 3×10^{-18} cm^2. Therefore, at a vapor density of 10^{17} atoms cm^{-3} of Li, the stopping distance for useful soft x rays is approximately 3 cm.

The metastable $Li^+(1s\,2s)^1S$ and $Li^+(1s\,2s)^3S$ population densities were determined by measuring the absorption of laser probe beams as a function of wavelength at the $Li^+[(1s\,2s)^1S\text{-}(1s2p)^1P]$ and $Li^+[(1s\,2s)^3S\text{-}(1s\,2p)^3P]$ transitions at 958.1 and 548.5 nm [Fig. 5(a)]. For this initial series of experiments a Quanta-Ray DCR-1 pulsed dye laser was used to produce the laser probe beams. While light at 548.5 nm was generated directly, a probe beam at 958.1 nm was produced by Raman downshifting the 685.2 nm output of the dye laser. The laser probe beam had a pulsewidth of approximately 5 ns and a linewidth of 0.5–1.0 cm^{-1}.

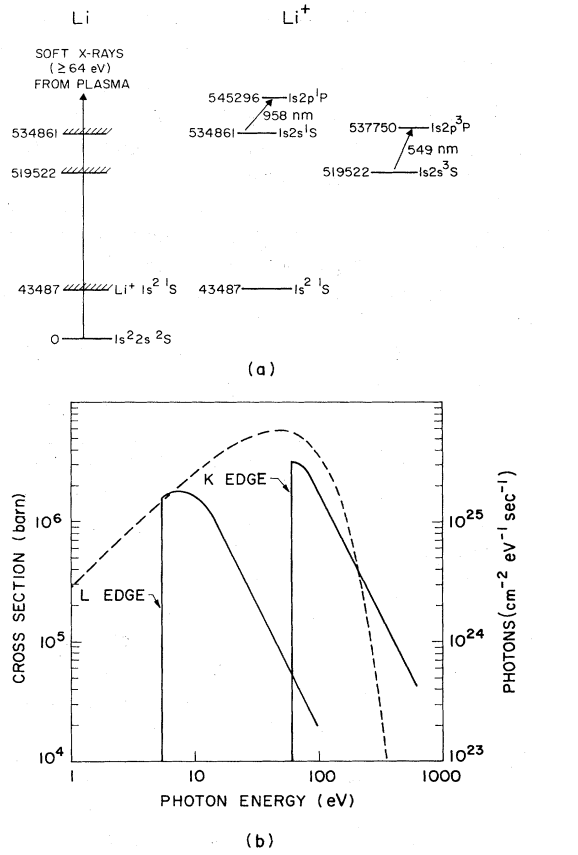

FIG. 5. (a) Energy-level diagram of Li and Li^+. The energies are in cm^{-1}. (b) Photoionization cross sections of Li (solid curve); emission spectrum of a 30-eV blackbody (dashed curve).

The absorption traces were fitted with numerically generated Voigt profiles and the integral of metastable populations over length along the probe beam was deduced. This process requires some knowledge of the transition oscillator strengths and the Doppler and Lorentzian components of the transition linewidth. The analysis of the $[(1s\,2s)^1S\text{-}(1s\,2p)^1P]$ absorption is straightforward, since the dominant contribution to the Lorentzian component of the linewidth of this transition is $\delta\omega_L \sim 0.13$ cm^{-1} from the natural lifetime of the upper level, which has a radiative decay in the vuv. The Doppler width and absorption oscillator strength of this transition are, respectively, $\delta\omega_D \sim 0.10$ cm^{-1} and $f \sim 0.21$. In the case of the $[(1s\,2s)^3S\text{-}(1s\,2p)^3P]$ transition, however, the dominant contribution to the Lorentzian component of the broadening comes from collisions with Li atoms and from Stark broadening. The numbers used in this analysis are derived from a simple calculation of the collision broadening[20] and from Ref. 21. In addition, the hyperfine structure of

the ^3S-^3P transition must be taken into account.[22] The total absorption oscillator strength for this transition is $f \sim 0.31$ and the Doppler width is $\delta\omega_D \sim 0.17$ cm^{-1}. The Lorentzian contribution to the linewidth of a particular component of oscillator strength f is given by $\delta\omega_L = (3.2\times10^{-17} n_e f^{2/3} + 0.015 f^{2/5})$, where n_e is the electron density (cm^{-3}) and the units of $\delta\omega_L$ are cm^{-1}. In this expression, the first term describes the contribution of Stark broadening,[21] while the second term describes that of "foreign gas" broadening.[20]

An example of the theoretical and experimental absorption traces obtained under one set of experimental conditions is shown in Fig. 6. It can be seen that the comparison of the theoretical curves with the experimental data is good. We estimate an accuracy of better than $\pm 50\%$ for the deduced value of the number density-length product, N^*L, of the Li$^+(1s\,2s)^1S$ ions and of a factor of approximately 3 for the ^3S ions. Strictly, the measured value of N^*L for either transition should be written as $(N_1 - N_2)L$, where N_1 and N_2 are the populations in the lower and upper levels of the transition in question. In the case of the $[(1s\,2s)^1S$-$(1s\,2p)^1P]$ transition, the short radiative lifetime (40 ps) of the upper ^1P level ensures an empty upper level. The same cannot be said for the $[(1s\,2s)^3S$-$(1s\,2p)^3P]$ transition. However, from the time evolution of the ^3S-^3P absorption—it can be deduced that the upper ^3P population is initially much smaller than the ^3S population. Thus the absorption technique yields a reasonable measurement of N^*L for the Li$^+(1s\,2s)^3S$ species for time delays of less than 4—6 ns between the probe and plasma-producing lasers.

In Fig. 7 is shown the observed dependence of integrated Li$^+(1s\,2s)^1S$ metastable population, N^*L, on the total laser energy incident on the target. The Li vapor density for this experiment was 10^{17} atoms cm^{-3}. The laser probe beam had a diameter of 2 mm and was centered about 1 mm from the Ta target (Fig. 2).

To deduce a value for the Li$^+(1s\,2s)$ metastable ion

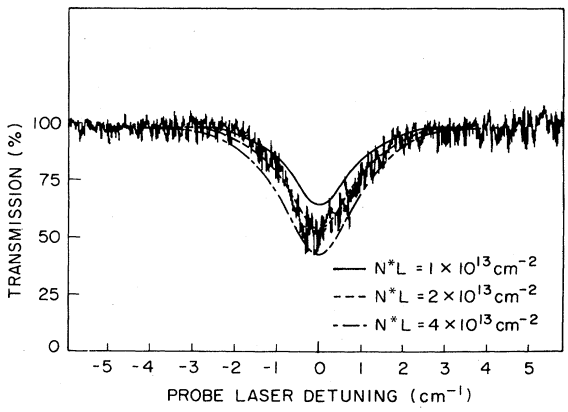

FIG. 6. Typical $[(1s\,2s)^1S$-$(1s\,2p)^1P]$Li$^+$ absorption trace. Laser energy on target ~ 50 mJ; probe-target distance ~ 1 mm; delay between probe laser and 1.06 μm laser peaks ~ 2—6 ns; Li atom density $\sim 10^{17}$ cm^{-3}. Superimposed are computer generated fits to the absorption trace: $\delta\omega_D \sim 0.1$ cm^{-1}; $\delta\omega_L \sim 0.13$ cm^{-1}; $f \sim 0.21$; probe laser linewidth ~ 1.25 cm^{-1}.

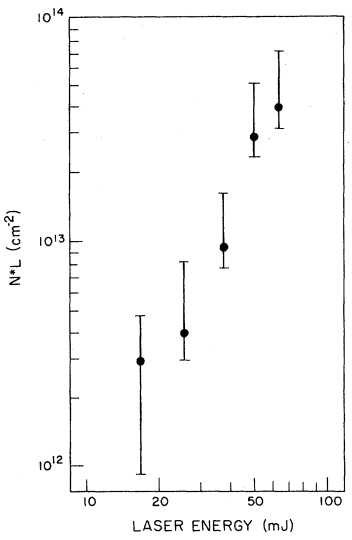

FIG. 7. Integrated metastable density, N^*L, for Li$^+(1s\,2s)^1S$ vs total laser energy incident on the target. Li vapor density $= 10^{17}$ cm^{-3}. The perpendicular probe-target distance is $R = 1$ mm. The time delay between the peaks of the probe and 1.06 μm lasers is ~ 4 ns.

population from the measurement of N^*L, it is necessary to decide on a particular spatial radiation pattern for the x rays emitted from the plasma. Now the plasma-producing laser is tightly focused to a spot with a 20 μm radius. At a typical plasma expansion velocity of 10^4—10^5 ms^{-1}, the plasma would move a distance of 5—50 μm during the 600 ps duration of the laser pulse. One would thus not expect the x rays to be emitted from the plasma with the Lambertian spatial distribution characteristic of emission from a plane surface. Rather, one would expect the relatively isotropic radiation pattern characteristic of emission from a spherical plasma.

Although the target was rotated between shots, after several revolutions of the target, a circular groove was created on the target corresponding to a region of plasma ablation. For subsequent shots the laser was focused into this groove and it is believed that this track resulted in a nonisotropic distribution of the x-ray emission. In the remainder of this work, it will be assumed that the x rays emitted from the plasma had the radiation pattern of a cone with a half angle of 45° and an axis normal to the target.

Given such a radiation pattern, integration yields the expression for the metastable ion density, N^*, at a distance R from the target of

$$N^* = 2(N^*L)/\pi R \ . \tag{1}$$

For the case of isotropic x-ray emission, the analogous expression would be

$$N^* = (N^*L)/\pi R \ . \tag{2}$$

Thus, assuming the conical radiation pattern, the maximum measured value of N^*L from Fig. 7 implies a Li$^+(1s\,2s)^1S$ population of 3×10^{14} ions cm^{-3}.

From the measurements recorded in Fig. 7, it is possible to make some deductions about the temperature of the plasma and the efficiency with which 1.06 μm radiation is converted to soft x rays. The metastable ^1S ion population density at a distance R from the target can be written as

$$N^*(R)=\int \frac{E_{BB}(\omega)\sigma(\omega)N_0}{\hbar\omega}\frac{d\omega}{2\pi R^2\beta}\ , \tag{3}$$

where N_0 is the ground-state Li atom density, $E_{BB}(\omega)$ is the energy radiated from the blackbody per unit bandwidth, and $\sigma(\omega)$ is the photoionization cross section for the production of $Li^+(1s\,2s)^1S$ metastable ions. For an isotropic radiation pattern, $\beta=1$, while $\beta=0.3$ for conical emission. Now the efficiency of conversion from 1.06 μm radiation to soft x rays can be defined as

$$\phi=\int E_{BB}(\omega)d\omega/E_L\ , \tag{4}$$

where E_L is the energy incident on the target from the main pulse of the laser output (in these experiments, 70% of the total laser energy incident on the target).

Making use of the Planck law, Eq. (3) can then be written in terms of a spectral overlap function, $S(T)$, as

$$N^*(R)=N_0\phi E_L\sigma_P S(T)/2\pi R^2\beta\ , \tag{5}$$

where

$$S(T)=\frac{1}{kT}\frac{\int_0^\infty x^2(e^x-1)^{-1}\kappa(xkT/\hbar)dx}{\int_0^\infty x^3(e^x-1)^{-1}dx} \tag{6}$$

and $\sigma(\omega)=\sigma_P\kappa(\omega)$ with σ_P being the peak photoionization cross section.

For the largest measured population from Fig. 7, $E_L=40$ mJ. Using the photoionization cross section of Ref. 18, with $\sigma_P=8.1\times10^{-19}$ cm^2, and assuming a conical radiation pattern ($\beta=0.3$), we find $\phi S(T)=1.4\times10^{15}$ J^{-1}. In Fig. 8 are plotted the spectral overlap function, $S(T)$, and the efficiency, ϕ (curve A), as functions of blackbody temperature. From these graphs it can be seen that the largest measured value of N^*L in Fig. 7 corresponds to an efficiency of conversion from 1.06 μm radiation to soft x rays in excess of 5%. Taking 70% as a reasonable upper limit to the value of ϕ,[23] these results yield an effective radiation temperature of 7–100 eV.

It should be noted here that the population measurements of Fig. 7 are taken at a time of 4 ns after the peak of the plasma-producing laser pulse. As discussed later, the population of $Li^+(1s\,2s)^1S$ ions was observed to decay under the conditions of Fig. 7 with a time constant of 3.6 ns. This would suggest a maximum value of $N^*L=1.2\times10^{14}$ at $t=0$, and thus a conversion efficiency determined by $\phi S(T)=4.4\times10^{15}$ J^{-1} (curve B). This would imply a conversion efficiency in excess of 17% and a blackbody temperature of between 9 and 70 eV.

These temperatures are lower than those observed[23–25] by other workers for incident laser intensities of 10^{13} W cm^{-2}. At typical plasma blow-off velocities,[2] it would be expected that heated plasma would move out of the 20 μm laser focal spot in a time shorter than the duration of the laser pulse. This would explain the relatively low radiation temperatures observed in this work in comparison with experiments,[4,23–25] at similar laser intensities, in which larger focal spot sizes or shorter laser pulses were involved.

Further confirmation of this explanation is given by the results shown in Fig. 9, in which N^*L is plotted as a function of distance of the focusing lens from the target. Also plotted is the measured intensity incident on target as a function of lens position. It can be seen that the measured value of N^*L changed by little more than a factor of 2 when the focusing lens was translated by ±3 mm, even though the estimated intensity at target changed by a factor of approximately 40. As the lens was translated, the focal spot size increased with the result that, although the laser intensity decreased, the hot plasma took longer to escape from the region of interaction with the laser. The net effect is thus relative insensitivity to the position

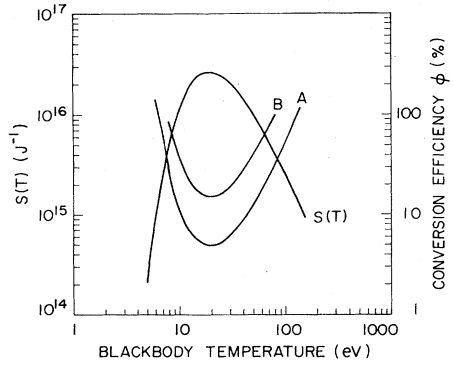

FIG. 8. $S(T)$ vs blackbody temperature and efficiency, ϕ, vs temperature for the cases: A, $\phi S(T)=1.4\times10^{15}$ J^{-1} and B, $\phi S(T)=4.4\times10^{15}$ J^{-1}.

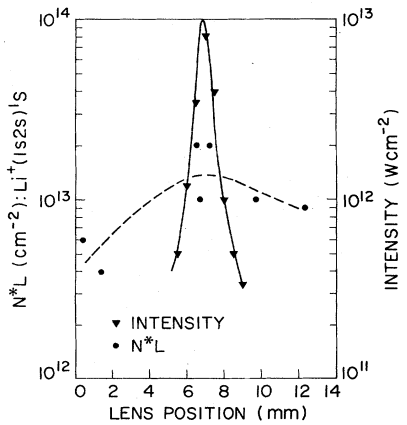

FIG. 9. Integrated $Li^+(1s\,2s)^1S$ density, N^*L, vs distance of lens from target. The zero is at an arbitrary position approximately 7 mm further from the target than the focal length of the lens. The total laser energy on target ~50 mJ; the probe beam-target distance ~1 mm; the delay between the 1.06 μm laser and probe laser peaks ~2–6 ns; the Li vapor density ~10^{17} cm^{-3}. Superimposed is the measured 1.06 μm laser intensity as a function of lens position.

of the lens.

From Eqs. (1) and (5) it can be seen that the value of N^*L is predicted to depend inversely on the value of R, the distance from the target. The observed dependence in these experiments was $N^*L \propto R^{-n}$ where n had a value of 0.7 ± 0.4. This is thus in rough agreement with theory.

Figure 10 shows the results of a measurement of N^*L for metastable Li^+ singlets as a function of the time delay, t, between the peaks of the 958.1 nm probe pulse and the 1.06 μm laser pulse incident on the Ta target. The time origin in Fig. 10 has an experimental uncertainty of ±2 ns. The slope of the graph corresponds to a singlet metastable $(1/e)$ decay time of 5.3 ns. Such a decay time is consistent with calculated rates[7] for destruction of Li^+ metastable ions due to collisions with electrons. At a probe-target distance of $R=1$ mm, the $(1s\,2s)^1S$ decay time was measured to be 3.6 ns. This change in decay time seems likely to be due to a somewhat higher electron density at $R=1$ mm than at $R=4.5$ mm, where the results of Fig. 10 were obtained. A similar measurement was made for the decay time of the $Li^+(1s\,2s)^3S$ state. A decay time of approximately 4—6 ns was measured under conditions that were the same as for Fig. 10—except for the probe-target distance which was 2 mm. In the case of the $Li^+(1s\,2s)^3S$ level, the observed decrease in the absorption on the $[(1s\,2s)^3S$-$(1s\,2p)^3P]$ transition could be due to either a decay of the ^3S level population or to an equilibration of the population in the $(1s\,2s)^3S$ and $(1s\,2p)^3P$ levels. It is unclear from this work which of these descriptions is correct.

The results of $Li^+(1s\,2s)$ population measurements presented so far are found to be quite well described by the expression

$$N^*L=(AN_0/R)\exp(-t/\tau) \tag{7}$$

for $t\geq4$ ns and $R\geq1$ mm. N^*, L, and R have units of cm^{-3}, cm, and cm, respectively, and N_0, the density of Li atoms, is in units of cm^{-3}. For metastable $Li^+(1s\,2s)^1S$ ions, $A=10^{-4}$ ions cm^2 and τ varies from 4—5 ns as R increases from 1 to 5 mm. For $Li^+(1s\,2s)^3S$ ions, $A=1.8\times10^{-3}$ ions cm^2 and $\tau=4$—6 ns at $R=2$ mm. The experimental uncertainty in the value of A is $\pm50\%$ for the ^1S ion and a factor of 3 for the ^3S ion. If a conical x-ray radiation pattern with a half angle of $\pi/4$ is assumed, the metastable ion density can be described by the expression

$$N^*=(BN_0/R^2)\exp(-t/\tau)\,, \tag{8}$$

where $B=6\times10^{-5}$ ions cm^2 for the ^1S ion and $B=1.2\times10^{-3}$ ions cm^2 for the ^3S metastable ion. In Eqs. (7) and (8), N^* should be replaced by the expression (N_1-N_2) for the case of the ^3S ion, where N_1 and N_2 are the populations in the ^3S and ^3P ion levels, respectively. Although it is believed that $N_2\ll N_1$ for $t<4$ ns, at later times this may no longer be the case.

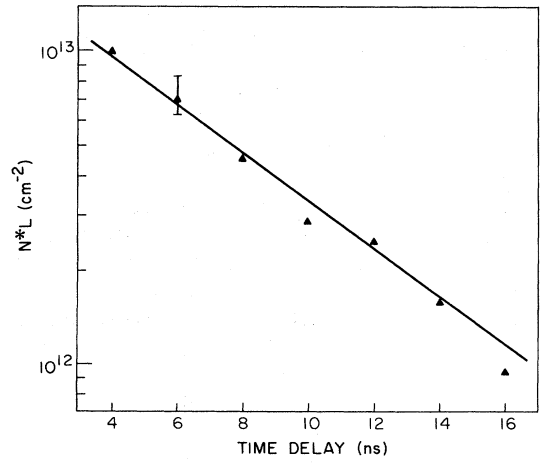

FIG. 10. N^*L for $Li^+(1s\,2s)^1S$ vs the time delay between the peaks of the probe laser and the 1.06 μm laser. Li vapor density $=10^{17}$ cm^{-3}; total incident laser energy ~50 mJ; $R\sim4.5$ mm.

B. Further investigation

In order to extend the results of the initial investigation, a second series of experiments was performed. In these experiments populations were measured using the dye laser system described in Sec. II C. The short pulse (600 ps) produced by this laser allowed measurements to be made at times closer to the time at which the x rays were emitted from the plasma. Because the dye laser amplifiers were pumped by radiation from the plasma-producing laser, there was no jitter between the arrival at the cells of the plasma-producing laser beam and the dye laser beam.

For these experiments the 1.06 μm laser beam was focused by a $f/16$ focusing system to an effective spot size of $\omega_0=30$ μm and an intensity on target of approximately 5×10^{12} W cm^{-2}. The output from the Nd:YAG laser system consisted of two pulses spaced by 4 ns—a main pulse and either a prepulse or a postpulse. The imaging system of Sec. II B was used in this second series of experiments. The size of the image of the plasma on the image plane was approximately 100 μm$\times$100 μm. The focus of the 1.06 μm beam could be reproducibly set to ±300 μm ($\pm0.1\%$ of the focal length of the lens) by monitoring the brightness of the image.

The first experiment performed with this improved apparatus was designed to investigate the effect on the plasma of a prepulse from the 1.06 μm laser. In Fig. 11 are shown measurements of the $Li^+(1s\,2s)^1S$ population as a function of time after the plasma-producing pulse was incident on the target. Measurements are shown that were taken under conditions of "no prepulse" (less than 1% of the main pulse energy) as well as under conditions of prepulses with energies of 30% and 70% of the energy of the main pulse.

For times earlier than the peak of the population ($t=0$), the presence of a prepulse resulted in a significant increase in $Li^+(1s\,2s)$ population. Later than $t=0$, however, there was no observable effect due to the presence or absence of a prepulse. It thus appears that no enhanced absorption of the main pulse occurred in the plasma due to the presence of the prepulse. This may be because the pulse separation of 4 ns is sufficiently long for the plasma produced by the prepulse to disperse before the arrival of the main pulse.

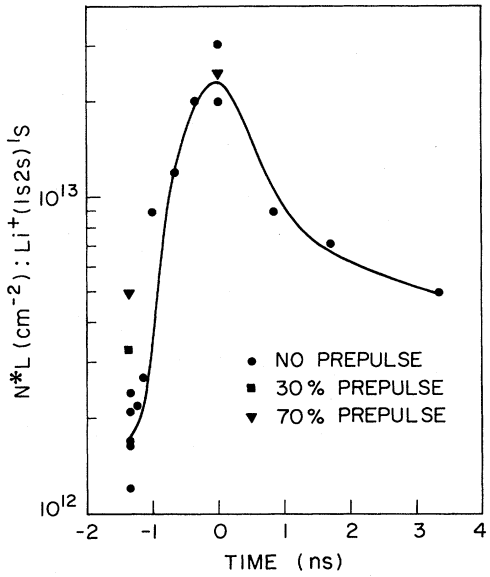

FIG. 11. Integrated $Li^+(1s2s)^1S$ density vs time delay between the peaks of the probe and 1.06 μm lasers for various prepulse conditions. Total incident laser energy $\sim$60 mJ, $R=2.5$ mm, Li density $=7.5\times10^{16}$ cm^{-3}.

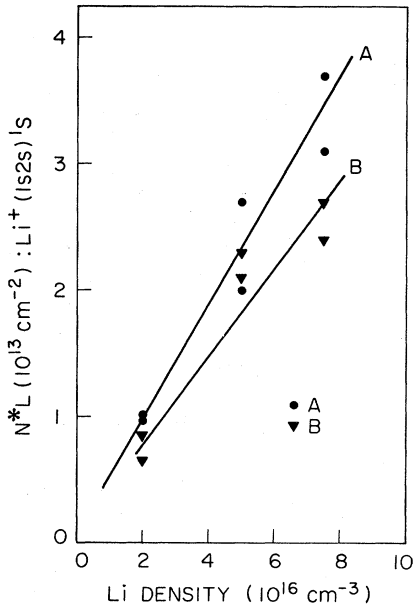

FIG. 12. Integrated $Li^+(1s2s)^1S$ density vs Li atom density. Total incident laser energy $\sim$60 mJ, $R=1$ mm, delay between the peaks of the probe and 1.06 μm lasers $\sim$1.5 ns.

It is instructive to compare the results of this measurement with the predictions of Eq. (7). At $t=3$ ns, Fig. 11 yields a value of $N^*L=5\times10^{12}$ cm^{-2}. Under conditions of $R=2.5$ mm and $N(\mathrm{Li})=7.5\times10^{16}$ cm^{-3}, Eq. (7) predicts $N^*L=2\times10^{13}$ cm^{-2}. The lower result measured here is believed to be due to the use of a less smooth target in this experiment than in the earlier work. The initial time decay in Fig. 11 is approximately 2 ns and is thus somewhat faster than that observed for $t\geq4$ in the earlier series of experiments.

In all subsequent experiments, the Nd:YAG laser was operated so as to produce a main pulse and a postpulse with energies of, respectively, 57 and 43 mJ. In Fig. 12 is shown the dependence of the number density-length product, N^*L, of $Li^+(1s2s)^1S$ ions on the Li density. The results of two separate experiments are shown, and in both a linear dependence on Li density can be observed. The different gradients of the two sets of data probably correspond to slightly different target conditions. It is interesting to compare these results with those of the initial series of experiments. From Fig. 12, at $t=1.5$ ns, $R=1$ mm and a Li density of 7.5×10^{16} cm^{-3}, an integrated density of $N^*L=3.5\times10^{13}$ cm^{-2} of $Li^+(1s2s)^1S$ ions was measured. Under these conditions, Eq. (7) would predict $N^*L=5\times10^{13}$ cm^{-2}. The agreement between the two series of experiments is thus quite good despite the difference in focusing geometries involved.

Making use of the earlier discussion on conversion efficiency and the results of Fig. 8 and Eq. (5), the measured population here, for $E_L=35$ mJ, corresponds to $\phi S(T)=2.0\times10^{15}$. This implies a conversion efficiency from 1.06 μm photons to soft x rays in excess of 7% and a plasma blackbody temperature of 7–95 eV.

At the low intensities used to produce the laser plasma in this work, the absorption of the 1.06 μm radiation is principally due to the process of inverse bremsstrahlung in the near critical density region of the plasma. The absorption coefficient for this process is linearly dependent on the charge of the predominant ionic species in the plasma. It is therefore preferable to use target materials with high atomic weights in order to allow the production of highly stripped ions in the laser-produced plasma. This consideration motivated the choice of tantalum as a target material in the initial experiments.

Other targets were used, however. Ni ($Z=28$) and Fe ($Z=26$) targets were tested. It was found that the $Li^+(1s2s)$ population excited when these targets were used was comparable, and 30–40% of that produced for the case of a Ta ($Z=73$) target. In all three of these cases the atomic weight of the target was relatively large and the difference was most likely due to subtle changes in the x-ray spectrum produced by these different elements.[25]

In contrast to these observations were the results obtained when a liquid Li ($Z=3$) target was used. When the target heater was turned off, liquid Li was able to condense on the Ta target. Under these conditions no $Li^+(1s2s)$ population could be measured. The scattered 1.06 μm radiation collected by the target imaging system increased by as much as an order of magnitude, suggesting a large decrease in the absorption of the incident 1.06 μm radiation by the plasma. These observations seem very reasonable in light of the low atomic number of Li and the correspondingly low maximum charge of the ions which could be produced in the plasma.

C. Long pulse plasma production

Since the $Li^+(1s2s)$ metastable ions have a measured deexcitation time of several nanoseconds under the condi-

tions of the experiments described so far, it seemed desirable to examine the production of these ions when the laser plasma was produced by a laser with a longer pulse duration. For this work, a commercially available Q-switched Nd:YAG laser was used. This laser operated at 10 Hz and produced 1.06 μm pulses with a triangular temporal shape and a foot-to-foot width of approximately 15—20 ns. The energy at the target was 200 mJ and an $f/8$ focusing system was used which resulted in a measured intensity on target of approximately 10^{12} W cm^{-2}.

By using the short-pulse dye laser to probe the $Li^+[(1s\,2s)$-$(1s\,2p)]$ transition, the $Li^+(1s\,2s)$ population could be observed during the Nd:YAG laser pulse. In Fig. 13 a set of data is presented which shows the development of the value of N^*L of the $Li^+(1s\,2s)^1S$ ion during the course of the plasma-producing pulse. The population reached a maximum at $t=0$, which corresponded to the peak of the Nd:YAG laser pulse, and then decreased rapidly. Clearly, the energy incident on the target during the second half of the pulse was not useful for creating $Li^+(1s\,2s)$ ions. One possible reason for this could be that the Li ground-state population was depleted by electron excitation to the Li^+ ground state and $Li(1s^2 2p)$ excited state on the time scale of a few nanoseconds. This would be in decided contrast to the results described earlier which were obtained with a 600 ps duration plasma-producing laser pulse. In those experiments no evidence of Li ground-state depletion was seen—an observation borne out by the measurements discussed in Sec. III D.

When a fresh target was placed in the cell, a similar temporal dependence of the value of N^*L was observed but the value of N^*L at $t=2$ ns was $N^*L \sim 8\times10^{12}$ cm^{-2}. Under the same conditions, at $t=2$ ns, the population excited when the plasma was produced by a laser pulse with a duration of 600 ps was $N^*L = 1.3\times10^{13}$ cm^{-2}. However, the on-target main pulse energy and intensity, for the case of the 600 ps laser pulse, were 40 mJ and 7×10^{12} W cm^{-2}.

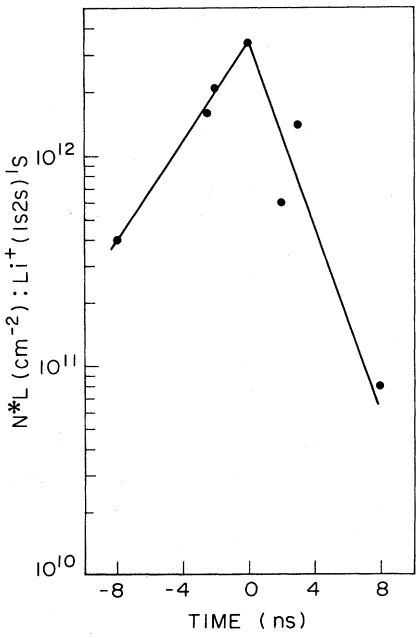

FIG. 13. Integrated $Li^+(1s\,2s)^1S$ density vs time for a plasma produced by a long-pulse 1.06 μm laser. Total incident laser energy $\sim$200 mJ; laser pulse is triangular with a base width of 15—20 ns; intensity on target $\sim10^{12}$ W cm^{-2}; $R=2$ mm; Li density $\sim7.5\times10^{16}$ cm^{-3}.

It can thus be seen that similar populations can be excited using commercial Q-switched lasers as with the more complex mode-locked system used in this investigation. However, more energy is required. This is in part due to the less focusable nature of the output beam and in part because of the long pulse length emitted from the Q-switched laser which appears, from the results of Fig. 13, to be largely wasted. It seems likely that a 1.06 μm laser pulse with a duration of 2—3 ns would be optimal for the excitation of the $Li^+(1s\,2s)^1S$ states under consideration here.

D. Population measurements: $Li(1s^2 2p)$; $Li^+(1s^2)$

In the process of producing the high densities of $Li^+(1s\,2s)$ ions measured in these experiments, comparable densities of electrons are created. These electrons subsequently lose energy due to inelastic collisions with Li atoms and, as a result, $Li(1s^2 2p)$ excited atoms and $Li^+(1s^2)$ ions are created. In this section, the results of measurements of the populations of these species are presented. The actively mode-locked Nd:YAG laser and short-pulse dye laser, described in Sec. II C, were used, respectively, to produce the plasma and to probe the excited-state populations. The focusing geometry of the 1.06 μm radiation was as discussed in Sec. III B.

In order to measure the population in the $Li(1s^2 2p)$ level, the probe dye laser was tuned through the $Li[(1s^2 2p)$-$(1s^2 3d)]$ transition at 610 nm. To deduce a value of the number density-length product, N^*L, for the $Li(1s^2 2p)$ level, from a measurement of absorption as a function of probe wavelength, some knowledge is required of the Lorentzian component of the transition linewidth. Under the conditions of these measurements, Stark broadening was a significant contributing mechanism to this linewidth. In the absence of detailed knowledge of the electron density in the photoionized region, it was thus difficult to obtain accurate $Li(1s^2 2p)$ population measurements from an examination of the absorption at 610 nm.

As discussed in Sec. II D, this problem can be avoided by using an interferometric technique to examine the refractive index of the system in the neighborhood of the 610 nm transition. In this way, using the technique of Duval and McIntosh,[15] satisfactory measurements of the $Li(1s^2 2p)$ population were obtained. Details of these measurements are reported elsewhere.[16]

In Fig. 14 the results of these measurements are presented as a function of distance from the target. It can be seen that, at a distance of 1 mm from the target, approximately 30% of the Li atom population has been excited to the $Li(1s^2 2p)$ states. The measurements of Fig. 14 were taken at a time of approximately 1.5 ns after the peak of the plasma-producing laser pulse. Under the conditions of this experiment, the $Li(1s^2 2p)$ population was

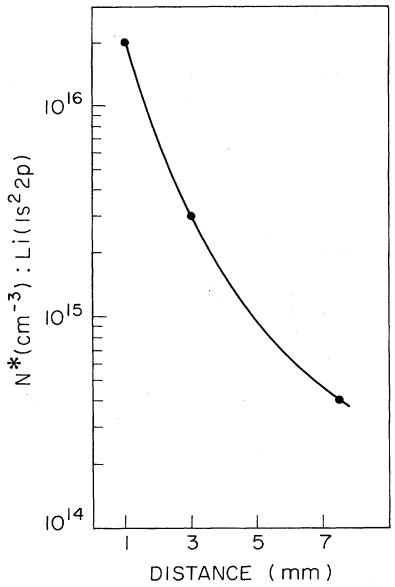

FIG. 14. Li($1s^2 2p)^2P$ population vs distance from target. Total incident laser energy $=70$ mJ; delay between probe and 1.06 μm lasers ~ 1.5 ns; Li atom density $\sim 7.5\times 10^{16}$ cm^{-3}.

observed to decrease with time roughly exponentially, with a time constant of 5—10 ns. The Li($1s^2 2p$) population in Fig. 14 has been obtained from the measurements of N^*L by making use of Eq. (1).

A measurement of the $Li^+(1s^2)$ ground-state ion population is complicated by the fact that the nearest excited level has an energy of approximately 60 eV. Because of this, neither the absorption measurements nor the inteferometric measurements utilized elsewhere in this investigation could be used. Instead, the $Li^+(1s^2)$ population was deduced from measurements of the electron density and the $Li^+(1s2s)$ population, with the assumption that only the $Li^+(1s^2)$ and $Li^+(1s2s)$ ion species contributed significantly to the number of electrons produced in the photoionized region.

To measure the electron density, the probe laser was tuned to the Li[($1s^2 2p$)-($1s^2 4d$)] transition at $\lambda=460.3$ nm. From measurements of the absorption as a function of wavelength in the region of this transition, it is possible[26] to deduce a value of ($N^*L\delta\omega_L$), where N^* is the population of the Li($1s^2 2p$) level and $\delta\omega_L$ is the Lorentzian component of the transition linewidth. Now, by means of the interferometric method of Duval and McIntosh,[15] the value of N^*L can be measured and thus the magnitude of $\delta\omega_L$ can be deduced. For this transition, the dominant contribution to the Lorentzian broadening is that of Stark broadening[21] and the electron density can thus be obtained from a knowledge of the magnitude of $\delta\omega_L$.

In this manner, using the Stark broadening coefficients from Griem,[21] the electron density was estimated to be $n_e\sim(1.2\pm0.6)\times10^{15}$ cm^{-3}. Under these conditions we measured integrated densities of $Li^+(1s2s)^1S$ ions of $N^*L=3.5\times10^{13}$ cm^{-2} and thus, from Eq. (1), populations of $N^*=2\times10^{14}$ cm^{-3}. If it is assumed that the ^1S and ^3S $Li^+(1s2s)$ ions are present in the ratio of their degeneracies, a total $Li^+(1s2s)$ population of 9×10^{14} cm^{-3} can be deduced. Hence, this assumption yields a population of $Li^+(1s^2)$ ions of 3×10^{14} cm^{-3}, with an upper bound of 1×10^{15} cm^{-3}. However, from the discussion of $Li^+(1s2s)^3S$ population in Sec. III A, the observed ratio of ^3S to ^1S $Li^+(1s2s)$ ions was approximately 18. In this case the total $Li^+(1s2s)$ ion density would be $(1-9)\times10^{15}$ cm^{-3} and there would have been no observable contribution to the electron density from the $Li^+(1s^2)$ ion. Therefore, we can only conclude that the Li^+ ground-state population was less than approximately 10^{15} cm^{-3}.

IV. SUMMARY AND DISCUSSION

From the results of this investigation it is clear that the use of soft x rays from a laser-produced plasma is a promising technique for producing large densities of metastable ions. Even with 50 mJ of 1.06 μm energy, densities of $Li^+(1s2s)^3S$ of 4×10^{15} ions cm^{-3} and of $Li^+(1s2s)^1S$ of 2×10^{14} ions cm^{-3} were produced at a distance of 1 mm from a tantalum target. The effectiveness of this excitation technique is well illustrated by the observation that these populations correspond to the excitation of 4% of the initial Li atoms to the metastable $Li^+(1s2s)$ levels with energies of approximately 60 eV. For comparison, in previous work using pulsed high power microwave discharges[27] and hollow cathode discharges,[28] metastable singlet densities of only 10^{11} ions cm^{-3} and 2×10^{12} ions cm^{-3}, respectively, were created.

Implicit to these results is the conclusion that, even at modest energies, the conversion efficiency from 1.06 μm energy to emitted xuv and soft x-ray energy is in excess of 5%. In this work the emitted radiation can be described as the emission from a blackbody with a temperature of 10—100 eV. Since the plasma-producing laser used in this work was a laboratory-sized instrument ($\sim$200 MW)—similar to commercially available models—which operated at repetition rates of up to 10 Hz, the laser-plasma represents an efficient and convenient source of intense radiation in the spectral region from 10 eV to 1 keV.

Finally, this work has established the importance of a geometry where the laser beam propagates through the ambient vapor. For a correct choice of laser wavelength and vapor density, the vapor, though completely ionized, will not substantially affect the focal spot size of the laser on the target.

Since the completion of this work, experiments of this type have been repeated in Na vapor, and population densities of $Na^+(2p^5 3s)^3P_2$ (at 33 eV) in excess of 10^{16} ions cm^{-3} have been produced. Also, Silfvast, *et al.*[29] have reported an experiment in which a 300 mJ pulse of 1.06 μm radiation from a Q-switched Nd:YAG laser was focused onto a target with an experimental geometry such as is described in this work. The soft x rays emitted from the plasma photoionized $4d$ electrons from Cd atoms in the ambient Cd atmosphere. Gains as large as 5.6 cm^{-1} were observed on the Cd^+ transition at 441.6 nm. Their experiments thereby demonstrate the first laser pumped by incoherent broadband soft x rays.

In considering the results of the experiments reported here, one particularly important result is the ratio of ex-

cited metastable Li ions to the number of ground-level ions. At an excited metastable $Li^+(1s\,2s)^1S$ density of $N^*=2\times10^{14}$ ions cm^{-3}, the ground-level $Li^+(1s)^2$ density is estimated to be less than 10^{15} ions cm^{-3}. The problem in inverting a system of this type results primarily from ground-level ions which are produced by hot photoionized electrons.[7,11] We believe that the system comes as close to inverting as it does as a result of the very rapid cooling of these hot electrons by resonance excitation of Li neutrals. At a Li density of 10^{17} atoms cm^{-3}, the total cooling rate for electrons[30–32] is approximately 260 eV ns^{-1}. Now at this Li density, the transition probability for ground-level ionization is 13 ns^{-1}, and so, a hot electron will produce, on average, 1.3 ground-level ions before cooling. We also note that, if an inversion were present, the measured metastable $Li^+(1s\,2s)^1S$ population, when transferred to the $Li^+(1s\,2p)^1P$ level, would correspond to a gain[7,11] at 199 Å of exp(3).

Several methods have been suggested for using metastable ion population for pumping what are in essence four-level laser systems.[33,34] These are based on using core-excited levels which lie above the lowest continuum and which are prohibited by selection rules from autoionizing. The lower level of these systems is a valence level of the atom or ion, which may either be empty, or may be emptied by an incident laser beam.

One example of such a system is shown in Fig. 15. In this system, photoionization by soft x rays would be used, as described in this paper, to produce metastable ionic population in the $Na^+(2p^5 3s)^3P_2$ level. At a neutral Na density of between 10^{17} and 10^{18} atoms cm^{-3}, 10% of this metastable population should transfer to the $Na(2p^5 3s\,3p)^4S_{3/2}$ level in several nanoseconds according to the charge transfer reaction

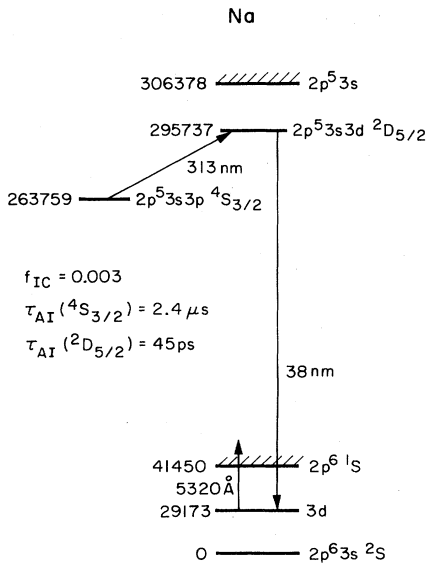

FIG. 15. Na xuv laser system.

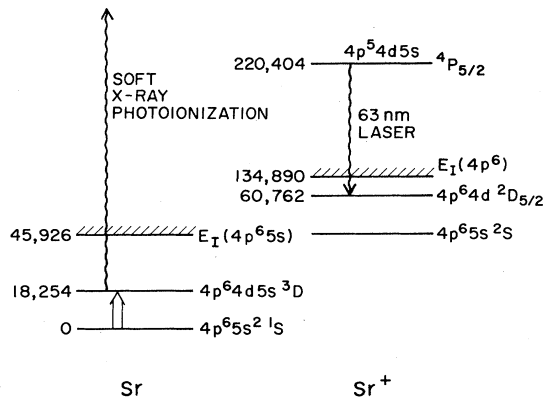

FIG. 16. Sr^+ xuv laser system.

$$Na^+(2p^5 3s)3P_2 + Na(2p^6 3s)^2S_{1/2}$$

$$\rightarrow Na(2p^5 3s\,3p)^4S_{3/2} + Na^+(2p^6)^1S_0 + 0.15\text{ eV}\ .$$

The $^4S_{3/2}$ level is itself metastable and is the only level, closer than several eV, to which the charge transfer reaction is exothermic. As described in earlier publications,[33,34] lasing would then be obtained by using an intense picosecond laser beam to transfer this population to a strongly allowed radiating doublet level.

A simpler and promising approach for using photoionization to realize an xuv laser is based on the concept of quasi-metastability of certain quartet levels of alkali-metal atoms and alkali-metal-like ions.[35] As a result of the selection rules for LS matrix elements, these quasimetastable levels, to first order, only couple to doublet basis levels which themselves are prohibited from autoionizing. In heavier elements these quasimetastable quartet levels mix sufficiently with the doublet series to have gain cross sections in the xuv of between 10^{-14} and 10^{-15} cm^2.

If one of the lower triplet levels of a group II metal is populated by either a laser or by electron excitation, then photoionization by soft x rays of atoms in this level will directly produce quartet atoms in quasimetastable levels of the group II ion. Figure 16 shows such a system in Sr^+. According to Hartree-Fock code calculations,[36] lasing would occur on the $Sr^+[(4p^5 4d\,5s)^4P_{5/2}$-$(4p^6 4d)^2D_{5/2}]$ transition at a wavelength of 62 nm and with a gain cross section of 10^{-14} cm^2. The lower laser level may, if necessary, be emptied by multistep ionization into Sr^{2+}. As a result of the many possible final levels that may be produced by photoionization, the fractional yield of $Sr^+(4p^5 4d\,5s)^4P_{5/2}$ quasimetastables from photoionized $(4p^6 4d\,5s)^3D$ Sr atoms is 7%. An assumed $Sr(4p^6 4d\,5s)^3D$ population of 10^{17} atoms cm^{-3} leads to a stopping distance of 1 cm for radiation at 27 eV—the peak of the photoionization cross section.[19] Based on the ideas developed in this paper, this in turn leads to a requirement of approximately 10 J of 1.06 μm laser energy to obtain a total gain of exp(25) for a twenty target-spot laser system.

ACKNOWLEDGMENTS

The authors gratefully acknowledge helpful discussions with R. W. Falcone and W. T. Silfvast and the computer programming of D. J. Walker and P. J. K. Wisoff, and thank Ben Yoshizumi for his many technical contributions. The work reported here was supported by the U. S. Office of Naval Research. One of us (R.G.C.) wishes to acknowledge the support of an IBM Postdoctoral Fellowship.

---

*Present address: Stanford Research Systems, Inc., 460 California Avenue, Palo Alto, CA 94306.

[1]C. Fauquignon and F. Floux, Phys. Fluids **13**, 386 (1970).

[2]P. K. Carroll and E. T. Kennedy, Contemp. Phys. **22**, 61 (1981).

[3]G. O'Sullivan, J. Phys. B **16**, 3291 (1983).

[4]M. D. Rosen, D. W. Phillion, V. C. Rupert, W. C. Mead, W. L. Kruer, J. J. Thomson, H. N. Kornblum, V. W. Slivinsky, G. J. Caporaso, M. J. Boyle, and K. G. Tirsell, Phys. Fluids **22**, 2020 (1979).

[5]R. G. Caro, J. C. Wang, R. W. Falcone, J. F. Young, and S. E. Harris, Appl. Phys. Lett. **42**, 9 (1983).

[6]M. A. Duguay and P. M. Rentzepis, Appl. Phys. Lett. **10**, 350 (1967).

[7]S. A. Mani, H. A. Hyman, and J. D. Daugherty, J. Appl. Phys. **47**, 3099 (1976).

[8]M. A. Duguay, in *Laser Induced Fusion and x-Ray Laser Studies,* edited by S. F. Jacobs, M. O. Scully, M. Sargent III, and C. D. Cantrell III (Addison-Wesley, Reading, Mass., 1976), p. 557.

[9]E. J. McGuire, Phys. Rev. Lett. **35**, 844 (1975).

[10]E. J. McGuire and M. A. Duguay, Appl. Opt. **16**, 83 (1977).

[11]H. A. Hyman and S. A. Mani, Opt. Commun. **20**, 209 (1977).

[12]H. Mahr and U. Roeder, Opt. Commun. **10**, 227 (1974).

[13]C. R. Vidal and J. Cooper, J. Appl. Phys. **40**, 3370 (1969).

[14]D. J. Kuizenga, IEEE J. Quantum Electron. **QE-17**, 1694 (1981).

[15]A. B. Duval and A. I. McIntosh, J. Phys. D **13**, 1617 (1980).

[16]R. G. Caro and J. C. Wang (unpublished).

[17]W. C. Marlow, Appl. Opt. **6**, 1715 (1967).

[18]G. Mehlman, J. W. Cooper, and E. B. Saloman, Phys. Rev. A **25**, 2113 (1982).

[19]E. J. McGuire, Phys. Rev. **175**, 20 (1968), and private communication.

[20]W. R. Hindmarsh and J. M. Farr, in *Progress in Quantum Electronics,* edited by J. H. Sanders and S. Stenholm (Pergamon, New York, 1972), Vol. 2, Part 3.

[21]H. R. Griem, *Plasma Spectroscopy* (McGraw-Hill, New York, 1964), p. 456.

[22]G. Herzberg and H. R. Moore, Can. J. Phys. **37**, 1293 (1959).

[23]H. Nishimura, F. Matsuoka, M. Yagi, K. Yamada, S. Nakai, G. H. McCall, and C. Yamanaka, Phys. Fluids **26**, 1688 (1983).

[24]D. L. Mathews, E. M. Campbell, N. M. Ceglio, G. Hermes, R. Kauffman, L. Koppel, R. Lee, K. Manes, V. Rupert, V. W. Slivinsky, R. Turner, and F. Ze, J. Appl. Phys. **54**, 4260 (1983).

[25]N. G. Basov, Yu. A. Bykovskii, A. V. Vinogradov, A. A. Galichii, M. P. Kalashnikov, V. L. Kantsyrev, Yu. P. Kozyrev, M. Yu. Mazur, Yu. A. Mikhailov, V. P. Puzyrev, A. V. Rode, G. V. Skliskov, and I. Ya. Frondzei, Sov. J. Quantum Electron. **12**, 977 (1982).

[26]A. Corney, *Atomic and Laser Spectroscopy* (Clarendon, Oxford, 1977), p. 300.

[27]J. R. Willison, R. W. Falcone, J. F. Young, and S. E. Harris, Phys. Rev. Lett. **47**, 1827 (1981).

[28]R. W. Falcone and K. D. Pedrotti, Opt. Lett. **7**, 74 (1982).

[29]William T. Silfvast, John J. Macklin, and Obert R. Wood II, Opt. Lett. **8**, 551 (1983).

[30]W. Williams, S. Trajmar, and D. Bozinis, J. Phys. B **9**, 1529 (1976).

[31]R. H. McFarland and J. D. Kinney, Phys. Rev. **137**, A1058 (1965).

[32]R. H. McFarland, Phys. Rev. **139**, A40 (1965).

[33]S. E. Harris, Opt. Lett. **5**, 1 (1980).

[34]Joshua E. Rothenberg and Stephen E. Harris, IEEE J. Quantum Electron. **QE-17**, 418 (1981).

[35]S. E. Harris, D. J. Walker, R. G. Caro, A. J. Mendelsohn, and R. D. Cowan, Opt. Lett. **9**, 168 (1984).

[36]R. D. Cowan, *The Theory of Atomic Structure and Spectra* (University of California Press, Berkeley, 1981), Secs. 8-1, 16-1, and 18-7.